Sigma J Eng Nat Sci, Vol. 44, No. 5, pp. 3246–3258, October, 2026

Sigma Journal of Engineering and Natural Sciences
Web page info: https://sigma.yildiz.edu.tr
DOI: 10.14744/sigma.2026.2157

Research Article

# The mechanical and modal characteristics of an aluminum-tourmaline metal matrix composite material

**Oğuzhan DAŞ[1,*], Hasan ÖZTÜRK[2], Zeki KIRAL[2], Binnur GÖREN KIRAL[2], Yeşim YÜCEL ÖZTÜRK[3], Bahadır UYULGAN[4], Batuhan DOĞDU[5]**

*[1]Department of Aeronautical Sciences, Turkish National Defense University, İzmir, 35410, Türkiye*
*[2]Department of Mechanical Engineering, Dokuz Eylül University, İzmir, 35390, Türkiye*
*[3]Department of Geological Engineering, Dokuz Eylül University, İzmir, 35390, Türkiye*
*[4]Department of Metallurgical and Materials Engineering, Dokuz Eylül University, İzmir, 35390, Türkiye*
*[5]CMS Wheels, İzmir, 35620, Türkiye*

## ARTICLE INFO

*Article history*
Received: 28 January 2025
Revised: 31 May 2025
Accepted: 14 July 2025

**Keywords:**
Aluminum Metal Matrix Composite; Damping; Modal Analysis; Tourmaline; Vibration

## ABSTRACT

This study explores the mechanical and dynamic properties of a novel aluminum-tourmaline metal matrix composite. While aluminum metal matrix composite materials are prized for their high strength and low weight, they may be dominated by excessive vibrations under dynamic environments, making their fundamental dynamic behavior and damping capacity essential to ensure reliability. To address this, an aluminum-tourmaline metal matrix composite was manufactured via stir casting, considering A356 aluminum alloy and 1% tourmaline by weight, and subjected to T6 heat treatment. The mechanical properties of the developed composite were determined according to DIN EN ISO 6892-1 standard. The dynamic behavior was evaluated through impact hammer testing on a 250 × 250 × 8 $mm^3$ plate to obtain its fundamental frequencies and assess the damping capacity. To validate the fundamental frequencies, a numerical analysis was also conducted in ANSYS Workbench. The findings revealed that the aluminum-tourmaline composite exhibits a 10% higher modulus of elasticity and a 47.50% improvement in damping capacity compared to the matrix A356 aluminum alloy. Moreover, the first ten natural frequencies of the composite material were consistently higher with increments ranging from 9.909 Hz to 129.440 Hz, depending on the vibration mode. The outcomes indicate that tourmaline mineral is an effective reinforcement material that can be considered for aluminum composites for use in challenging applications.

**Cite this article as:** Das O, Öztürk H, Kıral Z, Gören Kıral B, Yücel Öztürk Y, Uyulgan B, Doğdu B. The mechanical and modal characteristics of an aluminum-tourmaline metal matrix composite material. Sigma J Eng Nat Sci 2026;44(5):3246–3258.

***Corresponding author.**
*E-mail address: droguzhandas@gmail.com

*This paper was recommended for publication in revised form by Editor-in-Chief Ahmet Selim Dalkilic*

Published by Yıldız Technical University Press, İstanbul, Turkey
© Author. This is an open access article under the CC BY-NC license (http://creativecommons.org/licenses/by-nc/4.0/).

## INTRODUCTION

Researchers examined metal matrix composite materials by introducing a novel material or manufacturing technique. Some others measured the impact of the manufacturing parameters, matrix material, or reinforcement on the material, including its mechanical properties and micro/macrostructure. Among those specifications, the vibration characteristics of the material also stand as a critical asset in understanding its natural frequencies to avoid the phenomenon called resonance. In addition, comprehending the vibrational behavior of a material is also essential to unearth its acoustic properties to suppress the noise as much as possible. The literature comprises many studies related tao material properties and mechanical properties [1-8], dynamic properties [9, 10], and manufacturing methods [11, 12] of aluminum metal matrix composites manufactured by considering various reinforcements. Some recent related studies are briefly presented as follows.

Sri et al. [13] investigated the impact of the silicon carbide (SiC) and graphite (Gr) on the mechanical and dynamic properties of AA7075 hybrid metal matrix composite. For this purpose, they considered 5 wt.% of SiC and 2 and 4 wt.% Gr. They measured the material properties by scanning electron microscope (SEM), energy dispersive X-ray (EDS) spectroscopy, and X-ray diffraction (XRD) analyses. In addition, they measured the wear resistance and vibrational behavior of the material. Singh and Pal [14] examined the mechanical and damping properties of the titanium oxide ($TiO_2$) and nanocrystalline lithium titanate ($Li_4Ti_5O_{12}$) coated SiC-reinforced aluminum metal matrix. They manufactured the material via the stir casting method and characterized the material by field emission scanning electron microscope (FE-SEM), EDS, transmission electron microscope (TEM), and electron back-scattered diffraction (EBSD). They assessed the mechanical and thermal damping of the material, considering temperatures ranged from -100 to 400°C. Wang et al. [15] measured the damping effect of the Al particle layer on the Alp/7075 aluminum composite material manufactured via the hot rolling process. They found that the damping characteristics of the composite depended on interface damping, dislocation damping, and grain damping. Sri et al. [16] investigated copper (Cu) particulates on the frequency responses and damping ratios of the aluminum-copper metal matrix composites. They employed a stir casting method considering different Cu ratios up to 15 wt.%. They characterized the material by SEM. For each composite, they evaluated the first two modal frequencies and corresponding damping ratios. Matli et al. [17] examined the mechanical, thermal, and damping properties of nitinol (NiTi) – aluminum nanocomposites. For this purpose, they considered 0.5, 1.0, and 1.5 vol. % NiTi to investigate the microstructure, thermal, mechanical, and damping properties of the composite manufactured by microwave sintering and hot extrusion. Rozhbiany and Jalal [18] considered mortar ash, met coke ash, nano-fibrillated composite, and straw ash as reinforcement materials to investigate the mechanical properties, damping, and wear resistance of aluminum metal matrix composites. For this purpose, all reinforcement materials are considered with a constant ratio of 5 wt.%. The composites are manufactured by using the stir casting method, in which a modified two-step mechanical stirrer having three blades is placed at each step. Baburaja et al. [19] examined the acoustic and vibration characteristics of the aluminum metal matrix composites reinforced by silicon carbide, considering uniform and non-uniform thermal environments. For this purpose, they conducted free and forced vibration analysis of the composites. Both vibration and acoustic analyses are conducted in the ANSYS environment, regarding different boundary conditions and temperature fields. Wang et al. [20] investigated the damping characteristics of aluminum-carbon nanotube-reinforced metal matrix composite material. The analyses are conducted considering simulations based on an open-source code. Ye et al. [21] studied the effects of the particle size of SiC on the mechanical behavior of SiC-aluminum metal matrix composites. They considered SiC-reinforced aluminum metal matrix composites having 65 wt.% SiC particles whose average size ranges between 10 μm and 50 μm. The failure characteristics of the material are analyzed by an optical microscope (OM). They covered the yield strength, microstructure, and failure mechanisms regarding compressive loading. Abd El Aal et al. [22] investigated the mechanical behavior of the Al-$Al_2O_3$ and SiC metal matrix composites manufactured by high-pressure torsion (HPT) and powder metallurgy (PM). The mechanical and material properties of the composite are examined by considering the microstructure, density, and tensile fracture.

The reinforcement material determines the superiority in mechanical properties of such composites as well as sets their cost. Studies in the literature and MMCs practically in the industry are generally composed of silicon carbide, boron carbide, fly ash, graphite, tungsten, molybdenum, or some bio-based material such as coconut shell, eggshell, etc. [10, 13, 18, 23-27]. The purpose of coming up with such a variety in the reinforcement material selection is to lower the cost while keeping or increasing the mechanical superiority of the composites. Although such diverse reinforcement materials are considered, promising minerals such as tourmaline remain unexplored despite their potential.

Tourmaline is a common accessory mineral found in a wide variety of lithologies and mineral deposits, including granitic [28], sedimentary and metamorphic rocks [29], tourmalinites [30], and stratabound and stratiform mineral deposits [31]. Tourmaline formation lithology is in the form of massive tourmalinite and foliated quartz-tourmaline rock. This rock is characterized by successive quartz bands and fine-grained tourmaline with a thickness of 2-10 mm. Tourmalinites consist of conformable layers comprising primarily of quartz and abundant tourmaline; Tourmalinites with tourmalines of schorl (Fe-rich)- dravite (Mg-rich) series is an abundant rock type of the Menderes Massif of western Anatolia [32]. Tourmalinite has proven

to be an important stratigraphic key unit for many metallic mineral deposits [33]. Tourmaline can host various major and trace elements [34]. The basic formula of tourmaline can be written as $XY_3Z_6(T_6O_{18})(BO_3)\ V_3W$, where X = Na, Ca, K, vacancy; Y = $Fe^{2+,}$ Mg, $Mn^{2+,}$ Li, Al, $Cr^{3+}$, $V^{3+}$, $Fe^{3+}$, ($Ti^{4+}$); Z= Mg, Al, $Fe^{3+}$, $V^{3+}$, $Cr^{3+}$; T = Si, Al, (B); V = OH, O; W = OH, F, O [34]. The main compositional varieties of this mineral are magnesian (Mg-) tourmaline or dravite, iron (Fe)-rich tourmaline, commonly known as schorl, and alkali tourmaline or Li-rich elbaite. There is a continuous series between dravite and schorl and between schorl and elbaite, but there is an interval of immiscibility between elbaite and dravite.

While the aforementioned mechanical properties of tourmaline render it a promising reinforcement material for use in aluminum metal matrix composites, the influence of tourmaline as a reinforcement material for aluminum metal matrix composites has not been examined yet. To the best of the authors' knowledge, no studies have reported on the impact of tourmaline usage as a reinforcement material on the mechanical properties and dynamic behavior of aluminum metal matrix composites. Based on this motivation, this study presents an exploratory investigation into the material, mechanical, and vibrational properties of aluminum–tourmaline metal matrix composites. The main contributions of the study can be summarized as follows:

(i) The introduction of tourmaline as a reinforcement material for aluminum metal matrix composites for the first time.
(ii) An examination of the impact of the tourmaline on the yield strength, tensile strength, and elasticity in comparison to the aluminum material.
(iii) An investigation of the free vibration and vibration damping properties of the aluminum-tourmaline metal matrix composite material.

The remainder of this paper is organized as follows. Section 2 outlines the manufacturing and testing methodologies followed in this study. Section 3 presents the experimental results obtained from the experiments and numerical analysis. Finally, Section 4 discusses the results and draws conclusions based on the experimental findings.

## MATERIALS AND METHODS

This study aimed to develop an alternative composite material having better-damping characteristics than the aluminum (A356) material without a considerable trade-off regarding material density. Tourmaline is a promising material to be utilized as an additive in increasing vibration damping due to its material properties [35]. For this purpose, aluminum-tourmaline metal matrix composites were manufactured considering 1% wt to understand the initial effect of tourmaline. To constitute a homogeneous mixture, it was aimed to obtain powder-sized (below 2 mm) tourmaline particles. For this purpose, the tourmaline mineral was first crushed into pieces by jaw crushers, followed by grinding procedures via rod mill, bond mill, and roller mill, respectively. All specimens were manufactured through the stir casting technique as depicted in Figure 1(a). Before

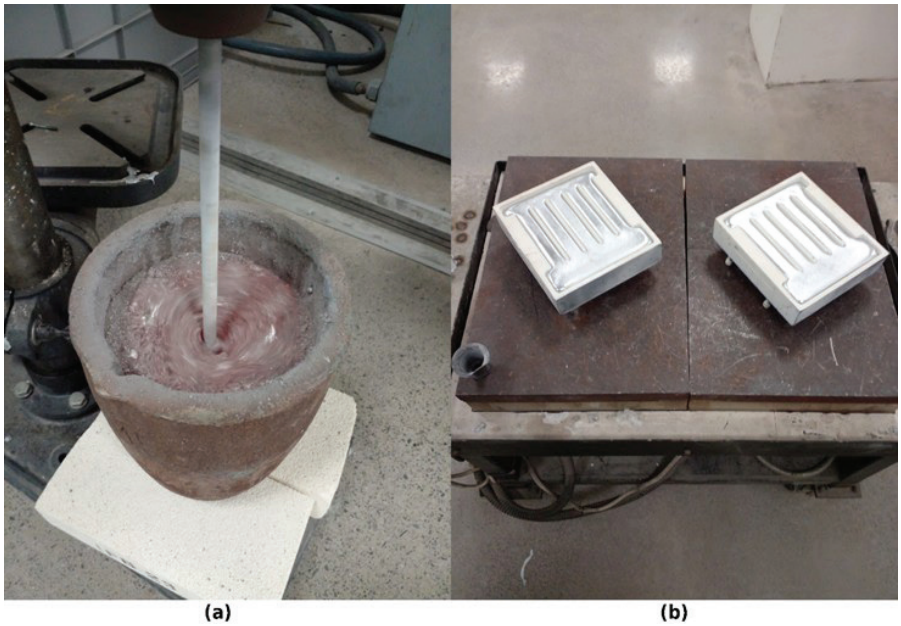



**Figure 1.** (a) The illustration of the stir casting procedure and (b) the poured material into the mold [36]. Adapted from Das O, Aybarc U, Yücel-Öztürk Y, Goren Kiral B, Ozturk H, Kiral Z, et al. A preliminary study on the manufacturing aluminum-potassium feldspar metal matrix composite materials. Mater Werkst 2023;54:109–119. https://doi.org/10.1002/mawe.202200100

casting, the reinforcement material was pre-heated at 750°C for 30 min. Afterwards, aluminum A356 was melted in the crucible at 750°C. The pre-heated reinforcement was poured into the vortex and stirred at 7 Hz for 2 minutes by an Optimum B20-400V mechanical stirrer to distribute the particles homogeneously. The material was poured into a mold shown in Figure 1(b), and preheated to 320°C. The specimens used for tensile testing and modal analysis are depicted in Figures 2 and 3, respectively. All specimens were subjected to T6 heat treatment where the material was solutionized at 540°C for 4 h, then quenched in water at 80°C, and aged at 155°C for 6 hours, artificially [36].

To obtain the mechanical properties of the manufactured materials, the tensile test specimens illustrated in Figure 2 were manufactured considering the DIN EN ISO 6892-1 tensile testing for metallic materials standard. The tensile tests were conducted based on this standard (5 mm/min tensile speed, 5N/mm$^2$ preloading under 10 mm/min loading speed) using the Zwick Roell Testing Machine to obtain the yield strength, tensile strength, modulus of elasticity, and the elongation of the materials. The test results are presented in Table 1.

The modal analysis was conducted for 250 × 250 × 8 mm$^3$ square thin plate specimens. The experimental modal analysis on that specimen was initiated using a PCB 086C01 modal impact hammer to obtain the impulse response of the plate. Three PCB352A24 model miniature accelerometers were used to obtain resonant frequencies as much as

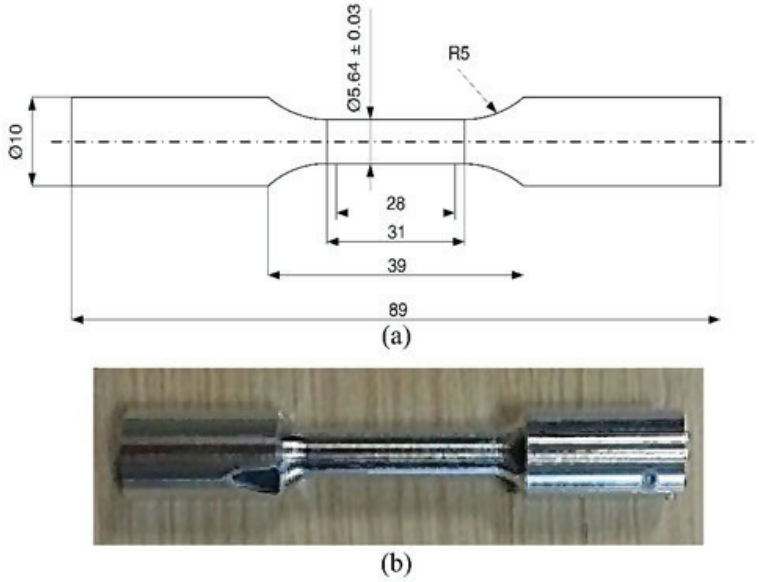



**Figure 2.** Tensile test specimen of aluminum-tourmaline metal matrix composite material (a) the dimensions (b) manufactured specimen.

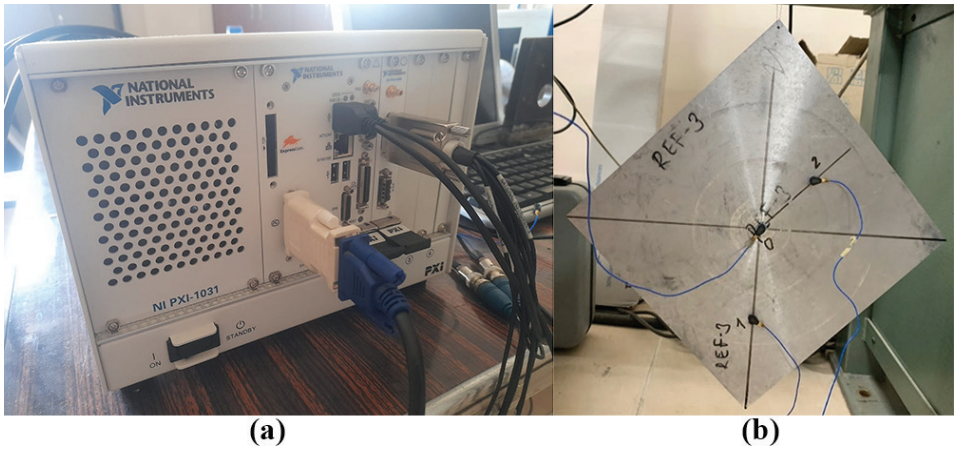



**Figure 3.** Experimental setup (a) data acquisition module and (b) the test square plate for experimental modal analysis.

**Table 1.** Mechanical properties of the manufactured aluminum-tourmaline metal matrix composite material

| Material | Additive Ratio (wt.) | Yield Strength (MPa) | Tensile Strength (MPa) | Young Modulus (GPa) | Elongation (%) |
|---|---|---|---|---|---|
| Aluminum (A356) | - | 182.52 | 251.30 | 69.97 | 6.01 |
| Aluminum-Tourmaline MMC | 1% | 180.50 | 251.00 | 76.19 | 6.34 |

possible through vibration signals sampled at 8 kHz using the NI PXI 4496 data acquisition system shown in Figure 3(a) in the LabVIEW environment. Each accelerometer has 100 mV/g sensitivity, 0.8 grams of mass, and can operate within a frequency range of 0.4 – 12000 Hz. The accelerometers were placed at the center (0), diagonal (1), and parallel (2) to the edge as depicted in Figure 3(b). All experiments were conducted with free boundary conditions satisfied by hanging the specimen with a nylon string.

The impact hammer modal analysis was performed in two sets, where the plate was excited ten times in each set using the impact hammer to get accurate results. The experimental natural frequencies and the corresponding response of the structure were obtained through the Fast Fourier Transform (FFT). The damping ability of the structure was interpreted by obtaining the damping ratio using the Exponential Envelope Curves (EEC). EEC involves analyzing the response of a system to a disturbance and fitting this response to an exponential decay model. The response of such a system can be displacement and velocity, although acceleration is the most common data considered for EEC. The envelope function of the exponential reduction of the data is obtained by the curve fitting method $x(t) = Ae^{-\zeta\omega_n t}$) where, A, $\omega_n$, $\zeta$, and t are amplitude, undamped natural frequency, damping ratio, and time, respectively. Figure 4 illustrates the free vibration response of a structure with a single degree of freedom. However, the plate examined in this study has multiple degrees of freedom, resulting in multiple damped natural frequencies. Among these frequencies, the first damped natural frequency is the most dominant and vibrations at this frequency decay more slowly compared to those at other frequencies. Consequently, the calculations for this study are based on the first damped natural frequency.

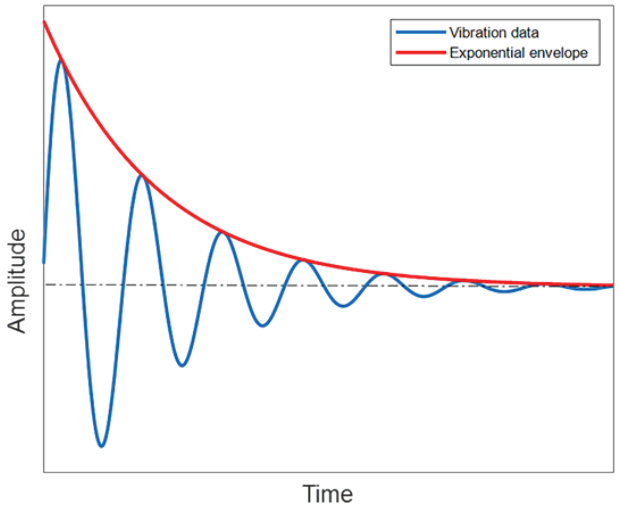



**Figure 4.** An illustration for the free vibration response of a system and its exponential envelope.

## RESULTS AND DISCUSSION

The accelerometer data collected from the impact hammer modal analysis were analyzed to obtain the response of the aluminum and aluminum-tourmaline MMC square plates. Among the twenty impacts (ten per test), the most representative data was chosen for the investigation. The most suitable acceleration data for both square plates are shown in Figures 5 and 6.

To understand how the natural frequencies and damping characteristics of aluminum were affected by the inclusion of the tourmaline mineral, the Fast Fourier Transform (FFT) of the accelerometer data belonging to aluminum and aluminum-tourmaline MMC plates was compared first. The FFT plots representing the vibration characteristics of those two plates are shown in Figures 7 and 8.

As seen in Figures 7 and 8, the first four natural frequencies of both plates were clearly observed in almost all accelerometer signals. To validate the results, the structure was modeled and analyzed through a modal analysis using ANSYS Workbench. For this purpose, a 20-node higher-order 3D element having three degrees of freedom called SOLID186 was considered. The modal analysis was conducted under free boundary conditions, which were also set for the experimental analysis. The convergence was obtained at 5022 elements and 28453 nodes.

For comparison and further analysis, the data collected from accelerometer #1 was considered since the first natural frequency values of both plates were barely or not visible in the FFT plots related to accelerometers #0 and #2. The validation analysis results are presented in Table 2 for the first four natural frequencies. The corresponding mode shapes were obtained as shown in Figure 9. It was observed that the first three modes were pure bending oscillations, while bending-torsional combined oscillations occurred at the fourth mode. The FFT plots of accelerometer #1 data were not depicted, only the first four natural frequencies. To make a detailed comparison between the aluminum

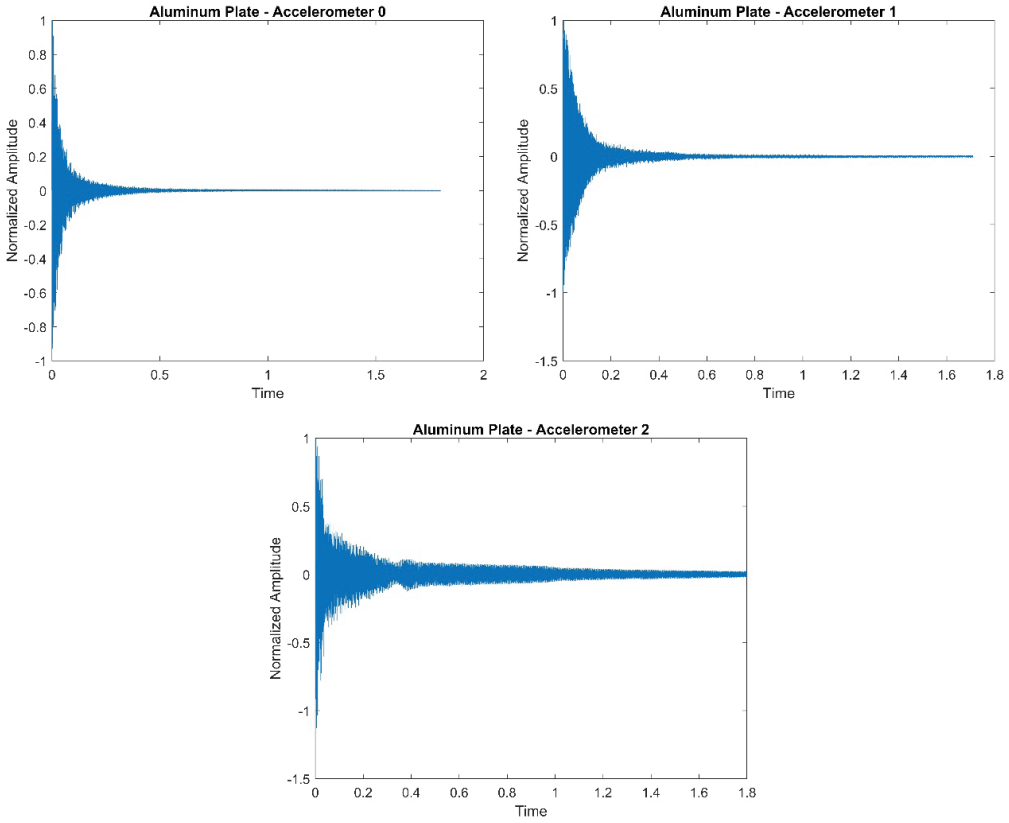



**Figure 5.** Accelerometer data related to the three accelerometers placed on the aluminum square plate.

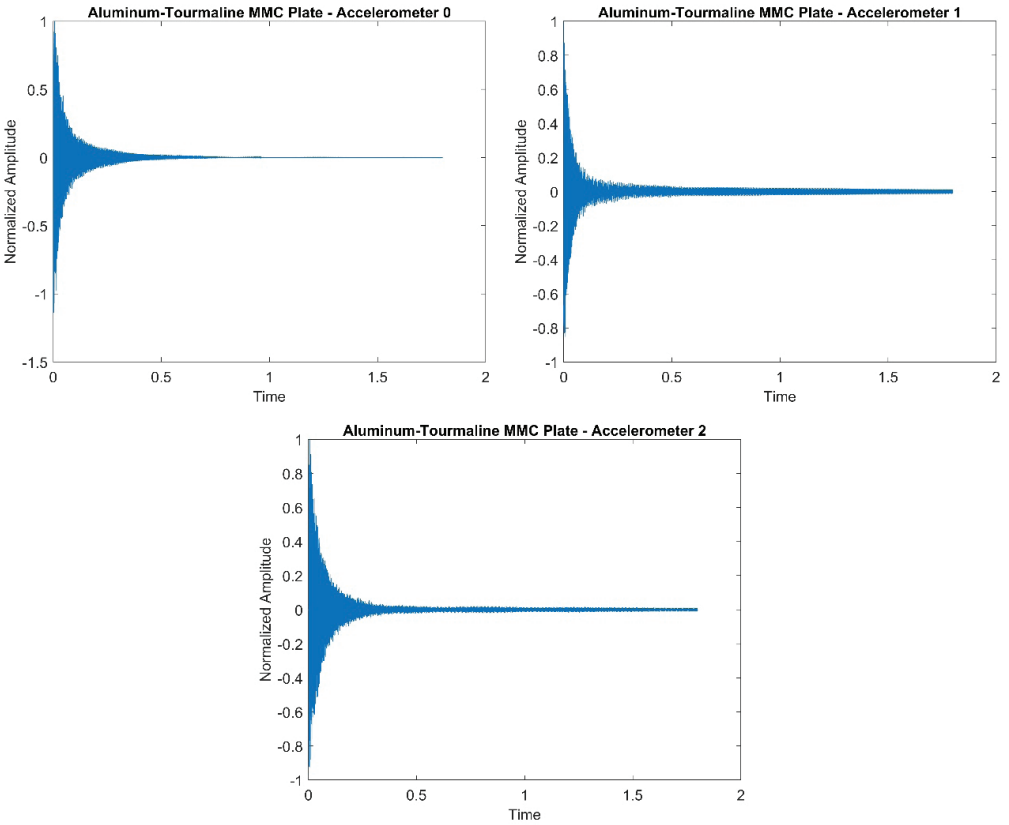



**Figure 6.** Accelerometer data related to the three accelerometers placed on the aluminum-tourmaline metal matrix square plate.

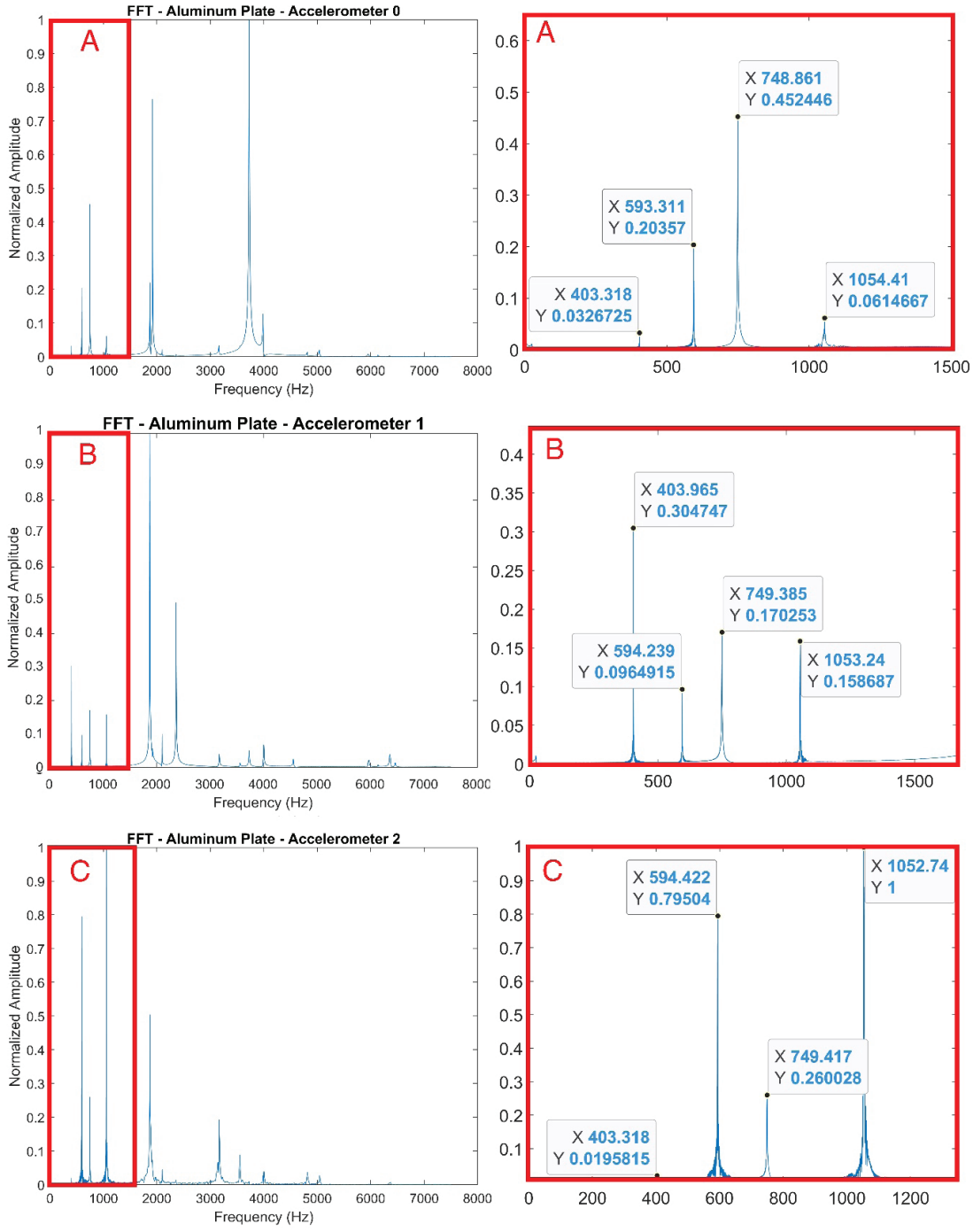



**Figure 7.** The FFT plots representing the vibration behavior of the aluminum square plate through (a) accelerometer #0, (b) accelerometer #1, and (c) accelerometer #2.

**Table 2.** The comparison of the computational and experimental (Accelerometer 1) modal analysis results

| Vibration Mode | ANSYS Workbench | Experiments | Difference |
|---|---|---|---|
| 1 | 413.130 Hz | 403.965 Hz | 2.18% |
| 2 | 607.530 Hz | 594.239 Hz | 2.18% |
| 3 | 751.950 Hz | 749.385 Hz | 0.34% |
| 4 | 1064.400 Hz | 1052.740 Hz | 1.09% |

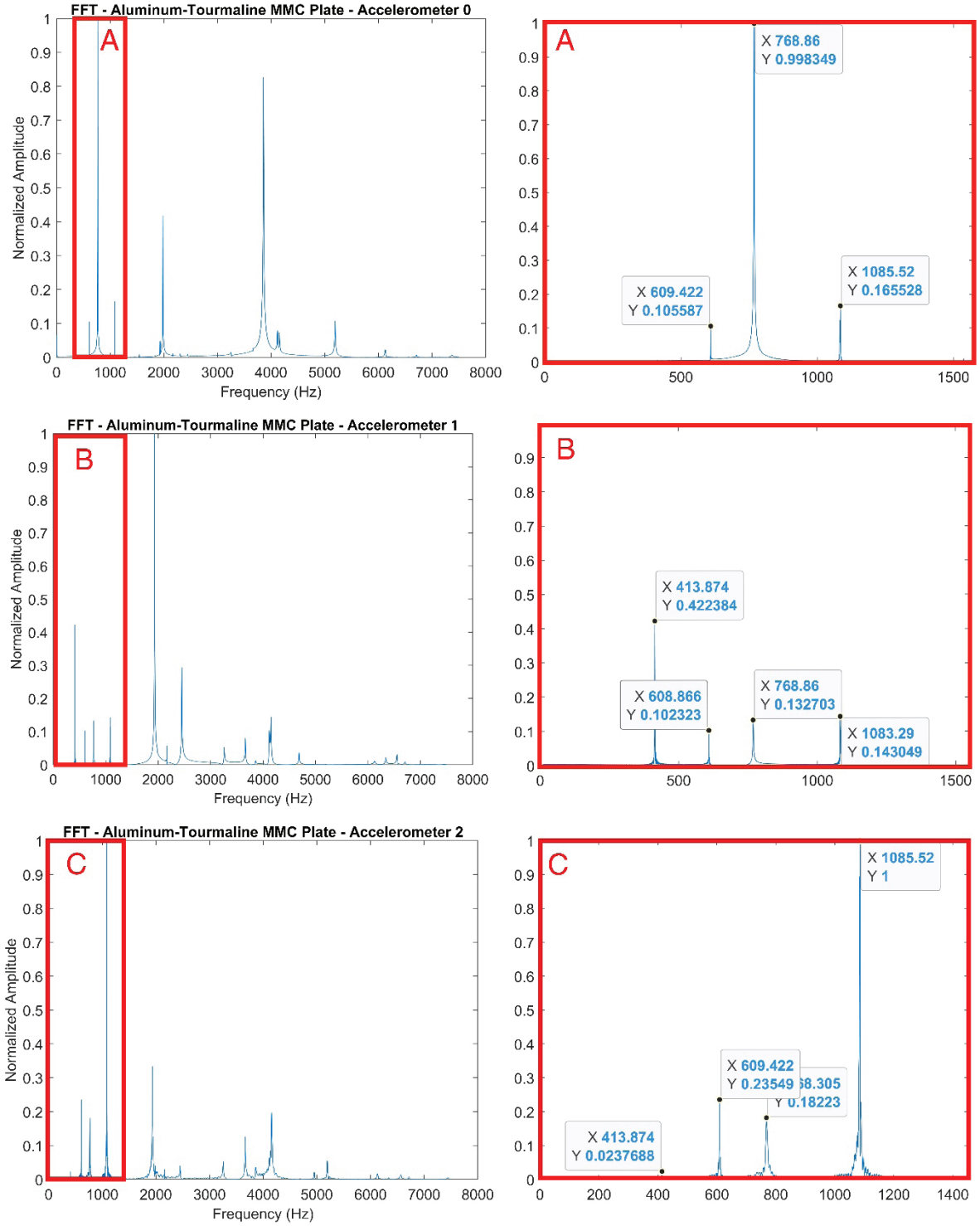



**Figure 8.** The FFT plots obtained for the aluminum-tourmaline MMC square plate through (a) accelerometer #0, (b) accelerometer #1, and (c) accelerometer #2.

and aluminum-tourmaline MMC square plates, the first ten natural frequencies and the corresponding normalized magnitudes of both plates obtained from the FFT analysis were compared in Figures 10 and 11.

The gap between the natural frequencies of the aluminum and aluminum-tourmaline MMC plates expanded incrementally from 9.909 Hz at the first natural frequency to 129.44 Hz at the tenth natural frequency. This discrepancy can be referred to as both the stiffness and the

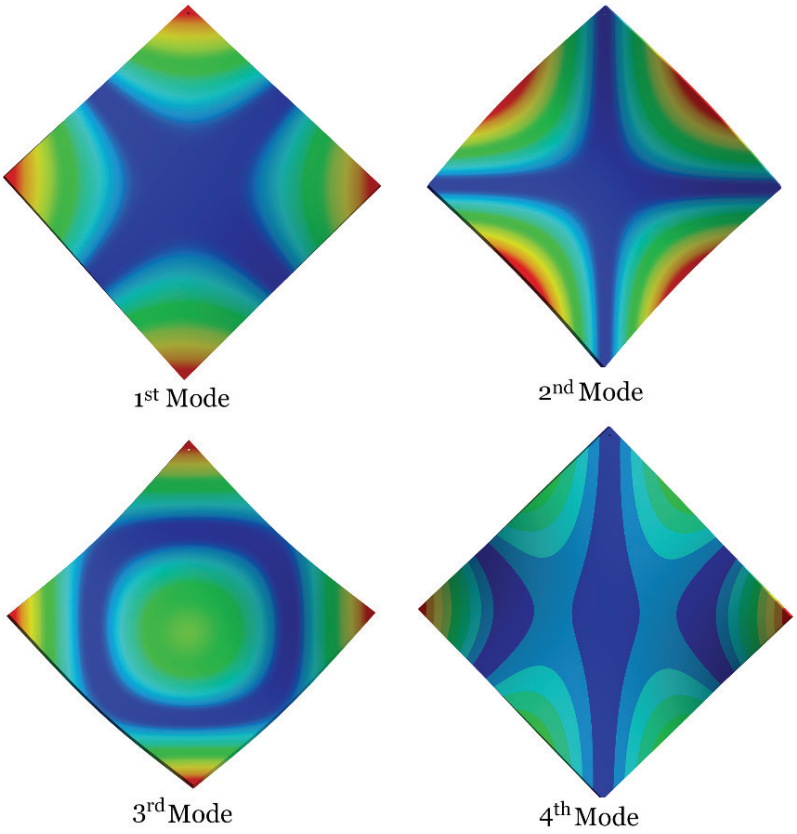



**Figure 9.** The first four mode shapes of the aluminum – tourmaline MMC square plate structure.

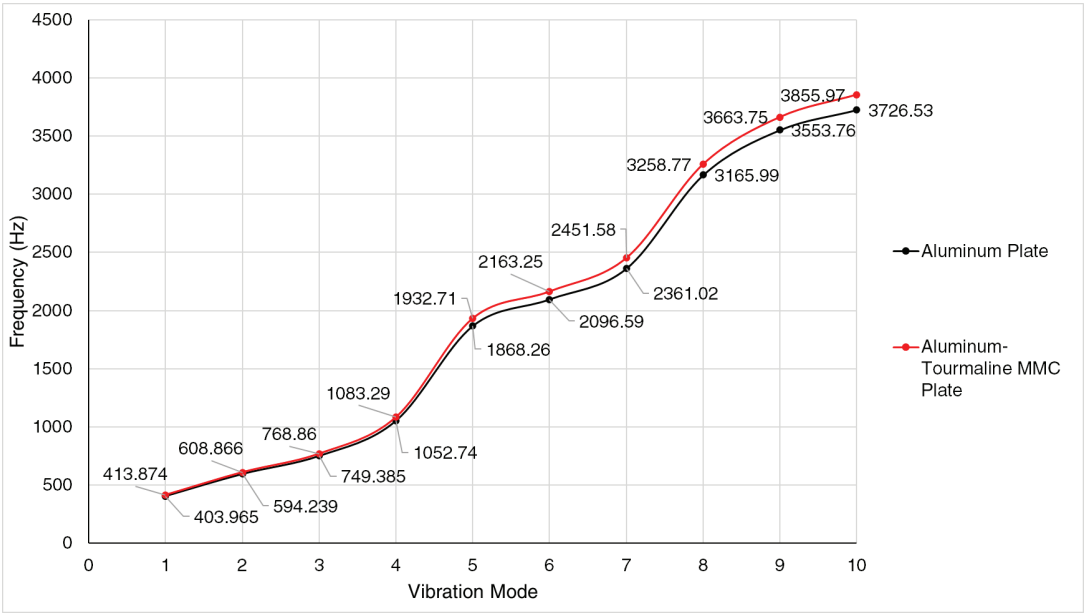



**Figure 10.** The first ten natural frequencies of the aluminum and aluminum-tourmaline MMC square plates.

mass density of the material. Since aluminum-tourmaline MMC has higher natural frequencies, it can be interpreted that it is stiffer because higher stiffness causes the plate manufactured by aluminum-tourmaline MMC to store and release process of energy at higher speeds, resulting in more frequent oscillations that increase its natural

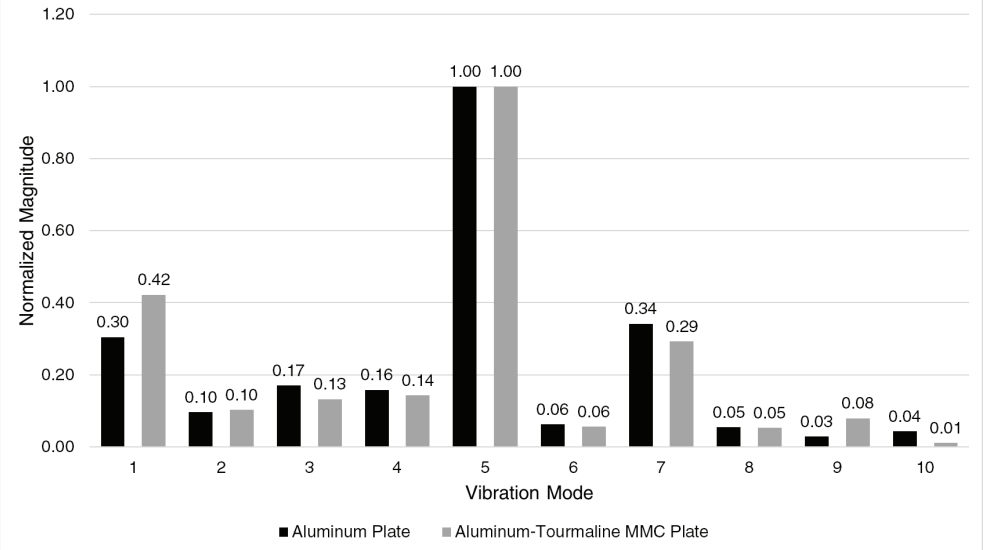



**Figure 11.** The normalized magnitude values per vibration mode obtained from the FFT analysis.

frequencies. Such an interpretation can be strengthened by noticing the higher modulus of elasticity observed for the aluminum-tourmaline metal matrix composite. For both structures, the dominant frequencies were obtained at the fifth mode, where the normalized responses were at their highest. Comparing the magnitude values for both plates, they exhibited a similar behavior as the magnitudes shown in Figure 11 were close to each other or equal. The difference between some magnitudes belonging to the first, third, fourth, seventh, ninth, and tenth modes may occur due to the nature of the modal impact test, where the excitation level depends on the expert who performs the test. Therefore, it would be more beneficial to make interpretations regarding the damping characteristics of the aluminum-tourmaline MMC plate by comparing its viscous damping ratio with the aluminum plate using exponential envelope curve fitting analysis. Figure 12 shows the exponential envelope and the viscous damping ratio of the reference aluminum and aluminum-tourmaline metal matrix composite plates for the first vibration mode.

As seen in Figure 12, the viscous damping ratio of the aluminum plate was lower by around 47.50% of than that of the aluminum-tourmaline MMC plate. Because the fundamental natural frequencies of both structures were close to each other and no mode shape changes were observed during computational analysis made in ANSYS, it can be stated that both structures dissipated the vibration at the same mode. Given the superior vibration damping and higher modulus of elasticity of the aluminum-tourmaline metal matrix composite, along with its yield and tensile strengths being nearly equal to those of the matrix, it can be concluded that the novel material retains its strength while achieving greater stiffness and improved vibration damping.

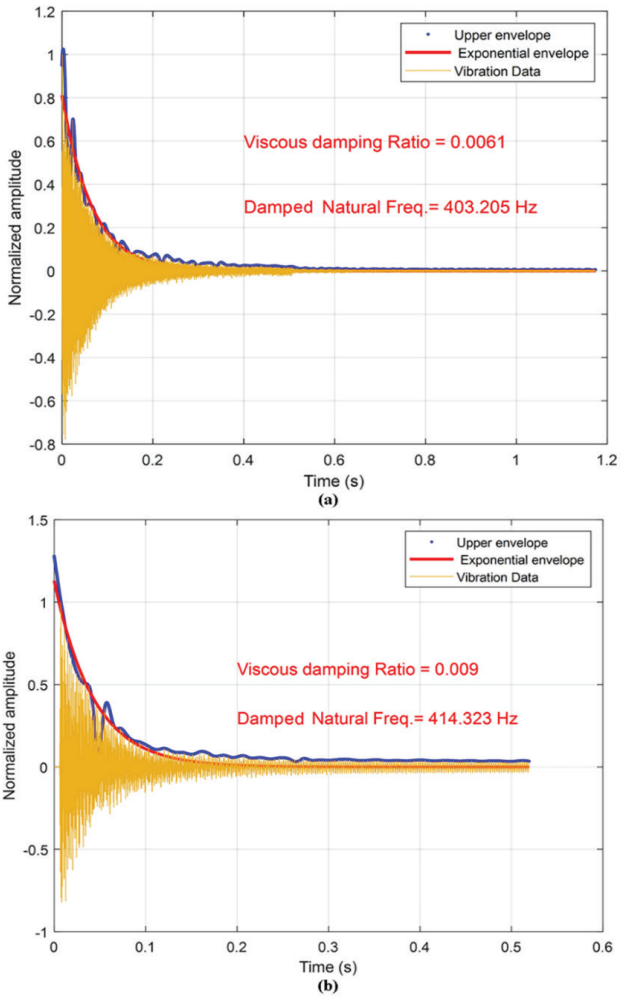



**Figure 12.** Exponential envelope curve of the acceleration data obtained from the accelerometer 1 placed on the (a) aluminum and (b) aluminum-tourmaline MMC square plates.

Compared with the few studies focused on the impact of SiC and Gr on the damping behavior [37, 38], tourmaline shows a great potential, specifically in terms of the damping capability of the composite material. For instance, the inclusion of SiC particles by 11.5% wt. resulted in approximately a 15-20% increment in damping capacity in AISI steel [37]. Similarly, inclusion of 20% wt. SiC with 40% wt. rice husk ash (RHA) resulted in around a 50% increment in tan delta damping capacity of A356 aluminum alloy [38]. Regarding Gr as a reinforcement material, it was found that the modal damping of aluminum decreases with the inclusion of Gr, depending on its amount [39]. Such reports underline the contribution of the tourmaline mineral in enhancing the damping behavior of the aluminum metal matrix composites.

## CONCLUSION

This study examined the impact of the tourmaline mineral on the vibration characteristics of an aluminum-metal matrix composite plate experimentally. The efficacy of the tourmaline mineral was measured by comparing the first ten natural frequencies, corresponding responses, and the viscous damping ratio of the aluminum-tourmaline MMC plate with that of one made by the aluminum used as the matrix material for such an MMC. The inclusion of tourmaline mineral as a reinforcement material into aluminum-metal matrix material resulted in a stiffness increment by approximately 10% compared to the stiffness of the matrix material, as interpreted from the increment in the first ten natural frequency values ranging from 9.909 Hz to 129.440 Hz, depending on the vibration mode. Additionally, tourmaline mineral increased the viscous damping ratio of the aluminum by 47.50%. Due to its higher stiffness and damping ratio, along with nearly equal tensile and yield strengths, it can be concluded that the developed aluminum-tourmaline metal matrix composite has the potential to be utilized in mechanical structures where high stiffness and damping are required. Tourmaline demonstrated promising outcomes as a reinforcement material, such that even 1% wt. resulted in significant contributions to the mechanical properties of aluminum metal matrix composites, considering the additives used for similar purposes. Although further analysis regarding detailed investigation of other mechanical properties of this MMC may be required, the outcomes of this study indicate that tourmaline can be utilized as a reinforcement material in aluminum MMCs, specifically where vibration damping is essential.

## ACKNOWLEDGEMENTS

This study was supported by the Research Project Grant (Project number: 2018.KB.FEN.045) from Dokuz Eylül University Scientific Research Projects (BAP). We also would like to thank CMS Wheels for their support.

## AUTHORSHIP CONTRIBUTIONS

Authors equally contributed to this work.

## DATA AVAILABILITY STATEMENT

The authors confirm that the data that supports the findings of this study are available within the article. Raw data that support the finding of this study are available from the corresponding author, upon reasonable request.

## CONFLICT OF INTEREST

The authors declared no potential conflicts of interest with respect to the research, authorship, and/or publication of this article.

## ETHICS

There are no ethical issues with the publication of this manuscript.

## STATEMENT ON THE USE OF ARTIFICIAL INTELLIGENCE

Artificial intelligence was not used in the preparation of the article.

## REFERENCES

[1] Fenghong C, Chang C, Zhenyu W, Muthuramalingam T, Anbuchezhiyan G. Effects of silicon carbide and tungsten carbide in aluminium metal matrix composites. Silicon 2019;11:2625–2632. [CrossRef]

[2] Liu S, Wang Y, Muthuramalingam T, Anbuchezhiyan G. Effect of $B_4C$ and $MoS_2$ reinforcement on microstructure and wear properties of aluminum hybrid composite for automotive applications. Compos B Eng 2019;176:107329. [CrossRef]

[3] Krishnan PK, Christy JV, Ramanathan A, Mourad AHI, Muraliraja R, Al-Maharbi M, et al. Production of aluminum alloy-based metal matrix composites using scrap aluminum alloy and waste materials: Influence on microstructure and mechanical properties. J Alloys Compd 2019;784:1047–1061. [CrossRef]

[4] Salih OS, Ou H, Wei X, Sun W. Microstructure and mechanical properties of friction stir welded AA6092/SiC metal matrix composite. Mater Sci Eng A 2019;742:78–88. [CrossRef]

[5] Saba F, Zhang F, Liu S, Liu T. Reinforcement size dependence of mechanical properties and strengthening mechanisms in diamond reinforced titanium metal matrix composites. Compos B Eng 2019;167:7–19. [CrossRef]

[6] Idusuyi N, Olayinka JI. Dry sliding wear characteristics of aluminium metal matrix composites: A brief overview. J Mater Res Technol 2019;8:3338–3346. [CrossRef]

[7] Bishnoi D. Pressure exertion and heat dissipation analysis on uncoated and ceramic ($Al_2O_3$, $TiO_2$ and $ZrO_2$) coated braking pads. Mater Today Proc 2023;74:774–787. [CrossRef]
[8] Muniamuthu S, Kumar KS, Raja K, Rupesh PL. Dynamic characterization of hybrid composite based on flax/E-glass epoxy composite plates. Mater Today Proc 2022;59:1786–1791. [CrossRef]
[9] Prasob PA, Sasikumar M. Static and dynamic behavior of jute/epoxy composites with ZnO and $TiO_2$ fillers at different temperature conditions. Polym Test 2018;69:52–62. [CrossRef]
[10] Acar E, Aydın M. Damping behavior of Al/SiC functionally graded and metal matrix composites. J Asian Ceram Soc 2021;9:578–585. [CrossRef]
[11] Parsons EM, Shaik SZ. Additive manufacturing of aluminum metal matrix composites: Mechanical alloying of composite powders and single track consolidation with laser powder bed fusion. Addit Manuf 2022;50:102450. [CrossRef]
[12] Panwar N, Chauan A. Fabrication methods of particulate reinforced aluminium metal matrix composite - A review. Mater Today Proc 2018;5:5933–5939. [CrossRef]
[13] Sri C, Saravanamurugan S, Shanmugasundaram A, Mohapatra S. Effect of SiC and Gr particles on the mechanical properties and dynamic characteristics of AA 7075 hybrid metal matrix composite. Mater Today Proc 2021;46:390–398. [CrossRef]
[14] Singh S, Pal K. Investigation on microstructural, mechanical and damping properties of $SiC/TiO_2$, $SiC/Li_4Ti_5O_{12}$ reinforced Al matrix. Ceram Int 2021;47:14809–14820. [CrossRef]
[15] Wang YB, Jiang HJ, Liu CY, Huang HF, Wei LL, Qin FC. Influence of Al particle layer on damping behavior of Alp/7075Al composites fabricated by hot rolling. J Alloys Compd 2021;882:160763. [CrossRef]
[16] Sri MNS, Anusha P, Madhav VVV, Saxena KK, Chaitanya CS, Haranath R, et al. Influence of Cu particulates on A356MMC using frequency response function and damping ratio. Adv Mater Process Technol 2023;10:745–753. [CrossRef]
[17] Matli PR, Manakari V, Parande G, Mattli MR, Shakoor RA, Gupta M. Improving mechanical, thermal and damping properties of NiTi (Nitinol) reinforced aluminum nanocomposites. J Compos Sci 2020;4:19. [CrossRef]
[18] Rozhbiany FAR, Jalal SR. The effectiveness of reinforcement and processing on mechanical properties, wear behavior and damping response of aluminum matrix composites. High Temp Mater Process 2019;38:927–939. [CrossRef]
[19] Baburaja K, Subbaiah KV, Arunkumar MP, Bhagat VS, Reddy RKK. Vibration and acoustic characteristics of aluminium silicon carbide metal matrix composite under uniform and non-uniform thermal environment. Silicon 2020;13:4715–4736. [CrossRef]
[20] Wang F, Li L, Tang H, Wang X, Hu Y. Damping of aluminum-matrix composite reinforced by carbon nanotube: Multiscale modeling and characteristics. Sci China Technol Sci 2023;66:1062–1074. [CrossRef]
[21] Ye T, Xu Y, Ren J. Effects of SiC particle size on mechanical properties of SiC particle reinforced aluminum metal matrix composite. Mater Sci Eng A 2019;753:146–155. [CrossRef]
[22] Abd El Aal MI, El-Fahhar HH, Mohamed AY, Gadallah EA. The mechanical properties of aluminum metal matrix composites processed by high-pressure torsion and powder metallurgy. Materials (Basel) 2022;15:8827. [CrossRef]
[23] Mutlu A, Çavdar U. Investigation of mechanical properties of copper-graphene composites in terms of production methods and additive ratios: A review. Sigma J Eng Nat Sci 2024;42:600–613. [CrossRef]
[24] Altuner HM, Topuz A. The effect of processing time on the diffusion bonding of a SiCp reinforced aluminum matrix composite with a 380 casting aluminum alloy. Sigma J Eng Nat Sci 2011;29:457–464.
[25] Almomani MA, Hayajneh MT, Al-Shrida MM. Investigation of mechanical and tribological properties of hybrid green eggshells and graphite-reinforced aluminum composites. J Braz Soc Mech Sci Eng 2020;42:45. [CrossRef]
[26] Kumar LJ, Vishwanatha JS, Ganjigatti JP, Irfan G, Thara R. Investigation of mechanical properties of Al6061 with reinforcement of coconut shell ash and graphene metal matrix composites. Mater Today Proc 2023;91:413–417. [CrossRef]
[27] Hemalatha S, Ramakkrishna R, Srinivasa Rao D. Mechanical characterization of aluminum-boron carbide composites. Mater Today Proc 2024;115:101–109. [CrossRef]
[28] Neiva AMR. Geochemistry of tourmaline (schorlite) from granites, aplites, and pegmatites from northern Portugal. Geochim Cosmochim Acta 1974;38:1307–1317. [CrossRef]
[29] Henry DJ, Guidotti CV. Tourmaline as a petrogenetic indicator mineral: An example from the staurolite-grade metapelites of NW Maine. Am Mineral 1985;70:1–15.
[30] Ethier VG, Campbell FA. Tourmaline concentrations in Proterozoic sediments of the southern Cordillera of Canada and their economic significance. Can J Earth Sci 1977;14:2348–2363. [CrossRef]
[31] Slack JF. Tourmaline associations with hydrothermal ore deposits. Rev Mineral 1996;33:559–643. [CrossRef]
[32] Yücel-Öztürk Y, Helvacı C, Palmer MR, Ersoy EY, Freslon N. Origin and significance of tourmalinites and tourmaline-bearing rocks of Menderes Massif, western Anatolia, Turkey. Lithos 2015;218-219:22–36. [CrossRef]

[33] Mittwede SK, Helvacı C, Karamanderesi IH, Kun N, Candan O. Modes and implications of tourmaline occurrence in the Menderes Massif, western Anatolia, Turkey. Geosound 1992:179–190.

[34] Dutrow BL, Henry DJ. Tourmaline: A geologic DVD. Elements 2011;7:301–306. [CrossRef]

[35] National Center for Biotechnology Information. PubChem patent summary for JP-2002249612-A. PubChem. 2024. Available at: https://pubchem.ncbi.nlm.nih.gov/patent/JP-2002249612-A. Accessed November 4, 2026.

[36] Das O, Aybarc U, Yücel-Öztürk Y, Goren Kiral B, Ozturk H, Kiral Z, et al. A preliminary study on the manufacturing aluminum-potassium feldspar metal matrix composite materials. Mater Werkst 2023;54:109–119. [CrossRef]

[37] Madeira S, Miranda G, Soares D, Silva FS, Carvalho O. Study on damping capacity and dynamic Young's modulus of aluminium matrix composite reinforced with SiC particles. Cienc Tecnol Mater 2017;29:e92–e96. [CrossRef]

[38] Taj A, Doddamani SS, Vijaykumar TN. Vibration analysis of aluminum graphite metal matrix composite. Int J Eng Res Technol 2017;6:1072–1078. [CrossRef]

[39] Gaikwad SP. Comparison of damping characteristics of aluminium A356.0 with respect to Al-SiC-RHA hybrid composite. Int J Eng Res Technol 2017;6:171–174.